J Solid State Electrochem (2004) 8: 585–591
DOI 10.1007/s10008-003-0487-4

ORIGINAL PAPER

E. Bertolo · J. A. Kilner · M. Sahibzada

Oxygen diffusion in $SrCe_{0.95}Yb_{0.05}O_{3-\delta}$

Received: 11 April 2003 / Accepted: 29 September 2003 / Published online: 8 May 2004

Abstract $^{18}O/^{16}O$ isotope exchange depth profiling (IEDP) combined with secondary ion mass spectrometry (SIMS) has been used to measure the oxygen tracer diffusivity of $SrCe_{0.95}Yb_{0.05}O_{3-\delta}$ between 800 °C and 500 °C at a nominal pressure of 200 mbar. The values of D^* (oxygen tracer diffusion coefficient) and k (surface exchange coefficient) increase steadily with increasing temperature, and the activation energies are 1.13 eV and 0.96 eV, respectively. Oxygen ion conductivities have been calculated using the Nernst–Einstein equation. The transport number for oxide ions at 769 °C, the highest temperature studied, is only ~0.05. Moreover, $SrCe_{0.95}Yb_{0.05}O_{3-\delta}$ has been studied using impedance spectroscopy under dry O_2, wet O_2 and wet H_2 (N_2/10% H_2) atmospheres, over the range 850–300 °C. Above ~550 °C, $SrCe_{0.95}Yb_{0.05}O_{3-\delta}$ shows higher conductivity in dry O_2 than in wet O_2 or wet H_2; below that temperature the results obtained for the three atmospheres are comparable. Dry O_2 shows the highest activation energy (0.77 eV); the activation energies for wet O_2 and wet H_2 are identical (0.62 eV).

Keywords High-temperature proton conductor · Isotope exchange depth profiling · Oxygen diffusion · Secondary ion mass spectrometry · Strontium cerate

Abbreviations

HTPC	high-temperature proton conductor
IEDP	isotope exchange depth profiling
SIMS	secondary ion mass spectrometry

Presented at the OSSEP Workshop "Ionic and Mixed Conductors: Methods and Processes", Aveiro, Portugal, 10–12 April 2003

E. Bertolo (✉) · J. A. Kilner · M. Sahibzada
Department of Materials, Imperial College London,
Prince Consort Road, London, SW7 2BP, UK
E-mail: emilia@ibises.org.uk
Tel.: +44-020-75946725
Fax: +44-020-75843194

Introduction

In 1981, Iwahara et al. [1] showed that some $SrCeO_3$-based materials exhibited good protonic conductivity in hydrogen-containing atmospheres at high temperature. A typical example of these proton conducting materials is $SrCe_{0.95}Yb_{0.05}O_{3-\delta}$. In the past two decades, owing to its good proton conductivity, this perovskite-type oxide has attracted considerable attention [2, 3, 4]. Several studies have reported the use of $SrCe_{0.95}Yb_{0.05}O_{3-\delta}$ in devices such as hydrogen pumps [5], mixed potential gas sensors for hydrocarbon detection [6] or catalytic sensors for detection of methane [7, 8].

High-temperature proton conductors (HTPCs) derive their ionic conductivity from the incorporation of protonic defects with reasonably high mobility. These protonic defects are not an essential part of the lattice, but are incorporated into the material by dissociative absorption of water molecules at high temperature. Depending on the experimental conditions, the transport properties of HTPCs are dominated by protons, by oxide ion vacancies or by electronic defects. For the complete characterization of HTPCs, it is essential to determine the nature of the charge carriers, their concentration and diffusivity. A good understanding of the conduction processes is a key issue to optimize the performance of the electrochemical devices based on these mixed ionic conductors.

Secondary ion mass spectrometry (SIMS) is a very powerful tool for surface analysis. This mass spectrometric technique is capable of providing surface elemental and chemical information with high degree of resolution. Combined with isotope exchange depth profiling (IEDP), SIMS can provide accurate values of ion tracer diffusion coefficients (D^*) and surface exchange coefficients (k).

In SIMS, the surface of the sample is bombarded by high-energy particles, so-called primary particles. This bombardment leads to the ejection (sputtering) of both neutral and charged (positive and negative) spe-

cies from the surface; the ejected species are called secondary ions. Secondary particles may include electrons, neutral species, atoms and molecules, as well as atomic and cluster ions. These secondary ions are attracted to the mass spectrometer, where they are separated according to their mass/charge ratio. The separated positive or negative secondary ions can be collected in different forms: as mass spectra, as depth profiles or line scans, or as distribution images of the sputtered surface. When they are collected as depth profiles or linescans, the technique allows the collection of compositional information as a function of depth below the surface, being very sensitive to very low concentrations.

In 1993, Oghi et al. [9] published a SIMS study of two samples of $SrCe_{0.95}Yb_{0.05}O_{3-\delta}$, one annealed in dry air and the other in wet hydrogen gas. The difference in the negative mass spectra of both samples, where the signals at $m/z = 18$ and 19 were higher for the sample annealed in wet conditions, led them to believe that those two signals could be assigned to the species $^{16}O^{1}H_2$ and $^{16}O^{1}H_3$, respectively. De Souza et al. [10, 11] have studied different proton conducting perovskites, including $SrCe_{0.95}Yb_{0.05}O_{3-\delta}$. In their work, they question the stability of such controversial species, and discuss the existence of mass interferences arising from ^{18}O and ^{17}O (naturally occurring oxygen isotopes) and ^{19}F, the latter due to the possibility of fluorine contamination, either from the fabrication process or from the cutting and polishing of the samples for SIMS analysis. Moreover, the paper includes some preliminary data on oxygen diffusion and surface exchange coefficients in the temperature range 1000–700 °C.

In the present work, the $^{18}O/^{16}O$ SIMS/IEDP technique has been employed to investigate oxygen transport in $SrCe_{0.95}Yb_{0.05}O_{3-\delta}$ in the temperature range 800–500 °C. Some attention has been paid to the negative mass spectra in the range $m/z = 16$–19. The contribution of oxygen ions to the total conductivity has been obtained using the oxygen diffusion coefficients (D^*) by means of the Nernst–Einstein equation. Moreover, we report the conductivity data for $SrCe_{0.95}Yb_{0.05}O_{3-\delta}$ in three different atmospheres: dry O_2, wet O_2 and wet H_2, in the temperature range 850–300 °C. Similarities and differences with previous studies published in the literature are discussed in some detail. Finally, some transport numbers at different temperatures have been estimated, by comparing the oxygen conductivity data calculated from the diffusion coefficients with the conductivity obtained using impedance spectroscopy.

Experimental

The $SrCe_{0.95}Yb_{0.05}O_{3-\delta}$ was a commercial powder provided by Praxair Specialty Chemicals. The powder was first uniaxially and then isostatically (300 MPa) pressed into discs. The discs were then sintered in air at 1350 °C for 6 h. Once sintered, the pellets obtained were ca. 2 mm thick and 10 mm diameter, with relative densities higher than 96%. X-ray powder diffraction was performed at room temperature; a continuous scan mode was used to collect 2θ data from 5 to 120° with a 0.01° step and a 0.12°/min scan rate. The instrument used was a Philips PW1700 series automated powder diffractometer, using Cu Kα radiation (40 kV, 40 mA) with a secondary crystal monochromator. The diffraction pattern obtained confirmed the existence of the expected orthorhombic perovskite structure [12], and no additional phases were detected.

For the electrical measurements, symmetrical electrodes were applied by painting both sides of the sintered discs with platinum paste (Engelhard); the paint was first dried at 120 °C for ca. 15 min, and then fired at 1000 °C for 30 min. Conductivity measurements were carried out by means of a.c. impedance spectroscopy under three different atmospheres: dry O_2, wet O_2 and wet H_2 (the latter consisting of a mixture of N_2/10% H_2), using a Solartron 1260 impedance/gain phase analyser. The measurements were performed between 850 and 300 °C, and over the frequency range of 0.01–10^7 Hz. Dry O_2 atmosphere was obtained by passing the gas through P_2O_5; wet atmospheres were obtained by bubbling the corresponding gas through deionized water at room temperature. Before starting the measurements, the sample was first equilibrated at 850 °C overnight under the desired atmosphere; measurements were performed while cooling.

The impedance spectra were analysed as follows. At temperatures higher than ~480 °C, only a semicircle corresponding to electrode processes could be observed, of capacitance $\sim 10^{-6}$ F. The total electrolyte resistance was thus determined from the high-frequency intercept of this arc with the real axis. At lower temperatures (< 480 °C), it was possible to observe two new semicircles corresponding to bulk ($C \approx 10^{-11}$ F) and grain boundary contributions ($C \approx 10^{-9}$ F), the latter always much smaller than the bulk arc. In this case, the total electrolyte resistance was taken as the distance along the real axis between the intercepts of both arcs.

For the IEDP/SIMS experiments, both surfaces of the discs were first abraded with silicon carbide paper (250, 600 and 1200 grades) and subsequently polished down to 0.25 μm finish with successive grades of diamond spray. The samples were then ultrasonically cleaned in absolute ethanol to remove residues. Prior to the anneal in $^{18}O_2$ tracer gas, the samples were annealed in research grade oxygen (99.996% purity) for periods of time one order of magnitude longer than the following tracer anneal time, to ensure equilibrium conditions were attained. Samples were then quenched to room temperature, the research grade oxygen removed, and $^{18}O_2$ introduced. Once again, the samples were rapidly heated to the anneal temperature, annealed for the required time, and quenched. The annealing temperatures were between 800 and 500 °C, and the nominal oxygen partial pressure was 200 mbar. During the anneals, the water content was lower than

2 ppm. For the mass spectra analysis, two more samples were prepared: one sample polished but not annealed, that was used as blank, and one sample annealed at 675 °C only in research grade oxygen, without any subsequent ^{18}O anneal.

The diffusion profiles and negative mass spectra were determined on an Atomika 6500 SIMS instrument with a 5 kV Ar^+ primary beam. Owing to the insulating character of the samples, a 1 kV electron beam was used to avoid surface charge build-up. In the determination of D^* and k, two different modes were employed. For diffusion profiles less than 10 μm, the equipment was operated in depth profile mode; a depth profile is obtained by continuously recording the intensities of the relevant ions as the primary beam erodes the sample. In our case, the area scanned by the ion beam was 210 μm×210 μm, and the crater depth was measured post-analysis using a surface profilometer.

When the diffusion profiles were greater than 100 μm, it was necessary to employ the linescan technique. The samples were cut perpendicular to the polished surfaces, and the newly revealed sections polished again down to 0.25 μm. These sections were mounted normal to the primary ion beam; a well-focused beam could then be traversed perpendicular to the original polished surfaces, and thus obtain the corresponding diffusion profiles. A more detailed explanation of the experimental procedure can be found elsewhere [13, 14].

Both D^* and k can be obtained by a non-linear least-squares fit of the experimental data to the solution of the equation:

$$C'(x) = \frac{C(x) - C_{bg}}{C_g - C_{bg}} = \operatorname{erfc}\left[\frac{x}{2\sqrt{D*t}}\right] - \left[\exp\left(\frac{kx}{D*} + \frac{k^2 t}{D*}\right) \times \operatorname{erfc}\left(\frac{x}{2\sqrt{D*t}} + k\sqrt{\frac{t}{D*}}\right)\right] \quad (1)$$

where $C(x)$ is the ^{18}O isotope fraction in the solid obtained by SIMS, C_{bg} the natural isotope concentration of ^{18}O, C_g the isotope enrichment of the annealing gas, and t the corrected time of the ^{18}O anneal.

Results and discussion

Sample characterization

Pellets of $SrCe_{0.95}Yb_{0.05}O_{3-\delta}$ were obtained by sintering at 1350 °C for 6 h; the relative density of the samples was higher than 96%. Powder XRD patterns obtained for sintered samples confirmed the existence of single phase material, with the expected orthorhombic perovskite structure. The microstructure of the sintered pellets was studied by scanning electron microscopy (SEM); one of the micrographs of an as-sintered surface is depicted in Fig. 1.

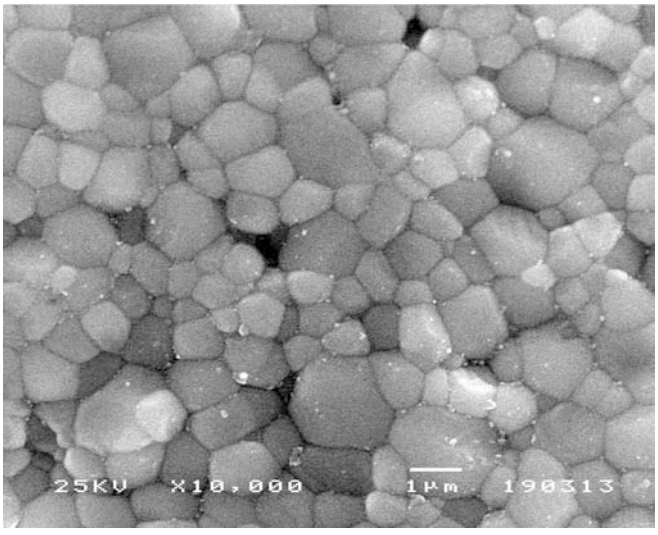

Fig. 1 SEM micrograph of $SrCe_{0.95}Yb_{0.05}O_{3-\delta}$ (as-sintered surface)

Conductivity measurements

Conductivity measurements were performed between 850 and 300 °C in dry O_2, wet O_2 and wet H_2 (10% H_2/N_2). Platinum paint was used as electrode material, and the measurements were performed while cooling, after equilibrating the sample overnight at 850 °C under the desired atmosphere. Figure 2 shows the temperature dependence of the total conductivity for the three atmospheres studied. Conductivity data obtained under dry O_2 are higher than those reported by Iwahara el al. [1] or Kosacki and Tuller [15], while for wet atmospheres the values compare well with those reported by other authors, such as Bonanos et al. [2]. It is noteworthy that, for temperatures above ~550 °C, $SrCe_{0.95}Yb_{0.05}O_{3-\delta}$ shows higher conductivity in dry O_2 than in wet O_2 or wet H_2, while for the wet atmospheres the conductivities are somewhat the same. However, below ~550 °C the results obtained for the three atmospheres are comparable. Dry O_2 shows the highest activation energy (0.77 eV); this E_a compares well with the value of ca. 0.80 eV, calculated from the data given by Kosacki and Tuller for dry O_2. The activation energies for wet O_2 and wet H_2 are identical, 0.62 eV, in line with the values reported by Bonanos et al. for air (0.65 eV) and N_2/5% H_2 (0.59 eV).

At high temperature and oxygen partial pressure, $SrCe_{0.95}Yb_{0.05}O_{3-\delta}$ behaves as a p-type conductor (hole conductor). However, when the material is exposed to water vapour, the contribution of hole conduction decreases and proton conduction appears; proton conduction thus predominates in both wet O_2 and wet H_2 atmospheres [16].

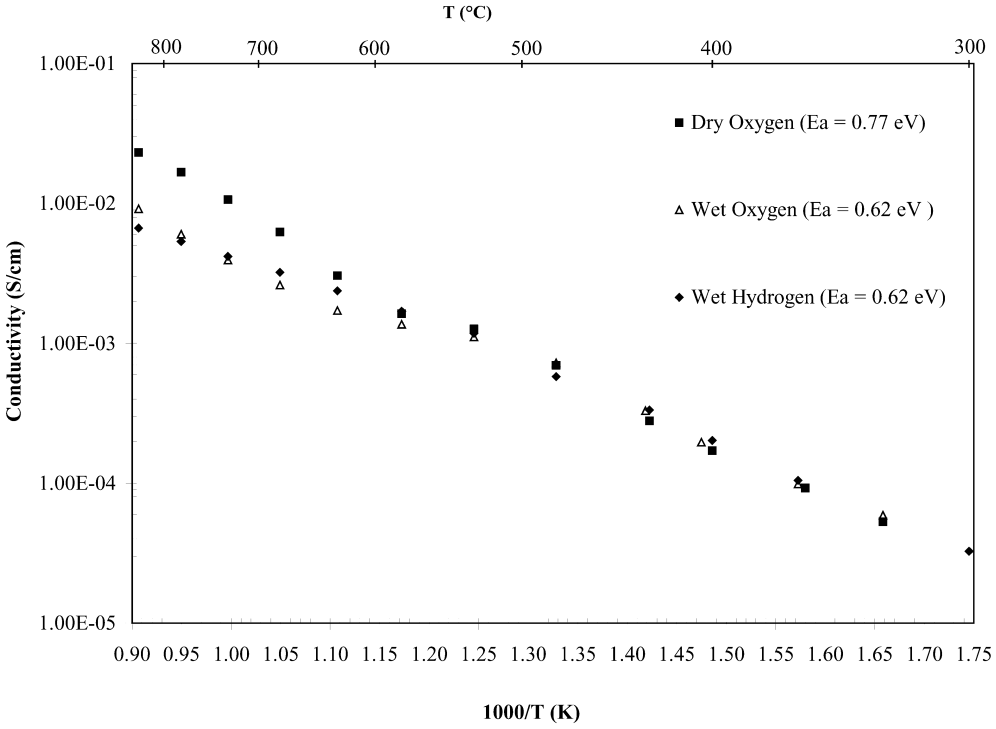

Fig. 2 Temperature dependence of the total conductivity for dry O_2, wet O_2 and wet H_2 (10% H_2/N_2)

IEDP/SIMS data

Negative mass spectra

Negative secondary ion mass spectra were obtained for one blank sample (not annealed), and for two samples annealed at 675 °C, one only in normal O_2 and the other one in oxygen enriched in ^{18}O. Selected secondary ions ratios, calculated from the spectra, are given in Table 1; the signals have been normalized with respect to the m/z 16 (^{16}O) signal. The interpretation of the signals in the mass range m/z 16–19 is complicated, due to the presence of mass interferences arising from the existence of three naturally occurring oxygen isotopes (^{16}O, ^{17}O and ^{18}O) and their respective OH_x^- species. In addition, De Souza et al. [10, 11] have pointed out the possibility of $^{19}F^-$ contamination.

However, a careful analysis of the different mass ratios provides some key information that is useful to identify the signals that appear in this mass range. First, the signal at m/z 18 can be assigned to $^{18}O^-$. The S_{18}/S_{16} ratio for both the blank sample and the one annealed in normal oxygen is identical to the $^{18}O/^{16}O$ natural isotopic ratio (0.2%), which means that there is no significant contribution from species such as $^{17}O^1H^-$ or $^{16}O^1H_2^-$. The S_{18}/S_{16} ratio for the sample annealed in $^{18}O_2$ is much higher (22%), as expected for a sample annealed in oxygen enriched in ^{18}O.

The S_{17}/S_{16} ratio in the blank sample is one order of magnitude higher than the natural isotopic ratio for $^{17}O/^{16}O$ (0.04%); however, the S_{17}/S_{16} ratio in the annealed samples falls considerably closer to the natural isotopic one. This decrease suggests that the signal at m/z 17 has a significant contribution from the species $^{16}O^1H^-$, and it is representative of bulk hydrogen; annealing in dry conditions thus removes protons from the samples. It must be pointed out that this signal cannot be utilized to quantify the proton concentration in the samples, since it has an important contribution due to residual gas absorption, depending on the primary ion beam current utilized [10]. In our case, all the samples were analysed under the same (high) beam current conditions.

Finally, the S_{19}/S_{16} ratio is identical for the three samples. If the signal at m/z 19 was due to the existence of $^{16}O^1H_3^-$, it would be reasonable to expect a decrease in the S_{19}/S_{16} ratio for the annealed samples, in a similar way to the one observed for the S_{17}/S_{16} ratio. The fact that the ratio remains unchanged seems more in agreement with the possibility of $^{19}F^-$ contamination, as suggested by De Souza et al., although further research will be necessary to ascertain the exact nature of this signal.

Table 1 Selected secondary ion ratios obtained from the negative mass spectra for a blank sample, and for the samples annealed at 675 °C in normal oxygen and $^{18}O_2$

	Blank sample (%)	Sample annealed in normal O_2(%)	Sample annealed in $^{18}O_2$ (%)
S_{17}/S_{16}	0.50	0.08	0.10
S_{18}/S_{16}	0.20	0.20	22.00
S_{19}/S_{16}	0.01	0.01	0.01

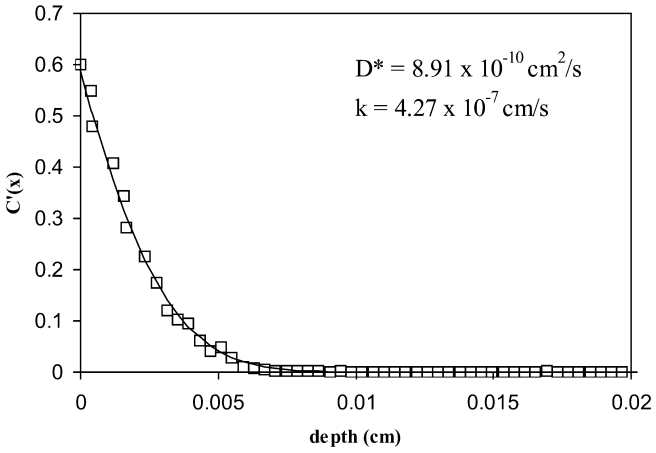

Fig. 3 Typical ^{18}O diffusion profile, showing the corrected isotope fraction vs. depth, together with the fitted curves (^{18}O anneal at 727 °C for 5419 s)

Oxygen diffusion data

Both D^* and k, in the temperature range 800–500 °C, have been obtained using $^{16}O/^{18}O$ IEDP/SIMS. A typical ^{18}O penetration profile is shown in Fig. 3; there is a good agreement between the experimental data and the fitted curve, which means that high quality diffusion data can be obtained by this method. Figure 4 depicts the Arrhenius plots for D^* and k, as well as the activation energies for each plot; values for D^* and k published by De Souza et al. [10] are also plotted in the same graph. In the temperature range where both studies overlap there is a reasonable agreement between the data published in this work and those of De Souza et al. The activation energies, obtained by regression analysis, are 1.13 eV for D^* and 0.96 eV for k.

The D^* coefficients can be used to calculate the oxygen ion conductivity by means of the Nernst–Einstein equation:

$$\sigma_o = \frac{Nq^2D*}{k_BT} \tag{2}$$

where q is the charge of the oxygen anion, k_B the Boltzmann constant and T the temperature; N is the number of oxygen anion sites per unit volume, and can be calculated from the structural data [12].

Figure 5 shows the resultant oxygen ion conductivity for $SrCe_{0.95}Yb_{0.05}O_{3-\delta}$, compared to the total conductivity data in dry O_2 obtained by impedance spectroscopy, as well as oxygen ion conductivity data published by Kosacki and Tuller [15], at $pO_2 = 1$ atm. The oxygen ion conductivity from this work is in general lower than the values published by Kosacki and Tuller, and the activation energy calculated (1.13 eV) is larger than the 0.77 eV published by these authors. This suggests that their conductivity data cannot be attributed solely to oxygen ion conduction, and could be related to mixed oxygen and proton transport.

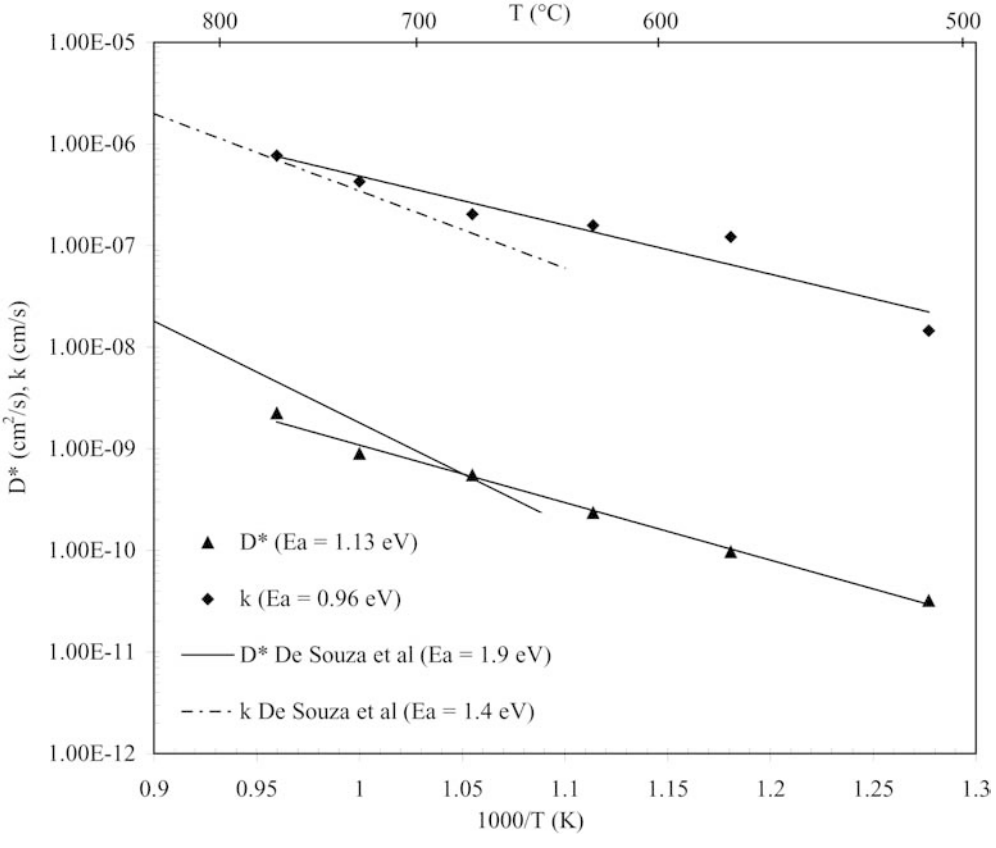

Fig. 4 Oxygen tracer diffusion coefficients (D^*) and surface exchange coefficients (k) as function of inverse temperature, at nominal O_2 pressure of 200 mbar. *Lines* are least-squares fits to Arrhenius behaviour

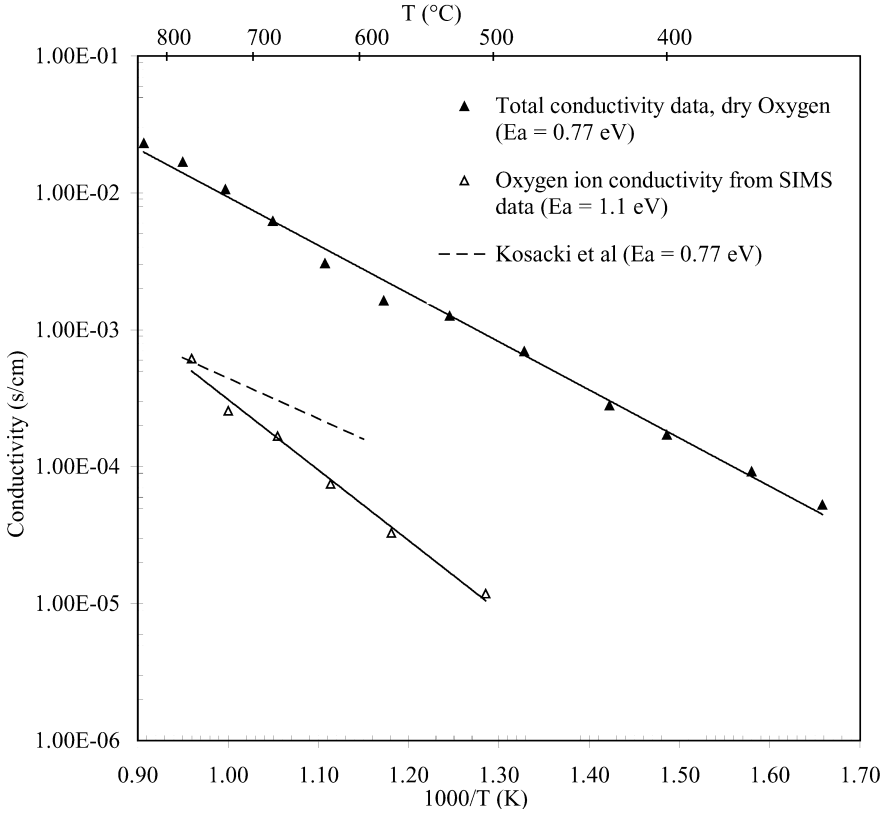

Fig. 5 Calculated oxygen ion conductivity obtained from SIMS data, total conductivity data determined by impedance spectroscopy in dry O_2, and oxygen ion conductivity data published by Kosacki and Tuller [15] at $pO_2 = 1$ atm

With the data obtained from the conductivity measurements, and the oxygen ion conductivity calculated from the SIMS data, it is possible to calculate transport numbers for oxygen (t_o) at different temperatures, with the equation:

$$t_o = \frac{\sigma_o}{\sigma_t} \tag{3}$$

where σ_o and σ_t are oxygen ion conductivity and total conductivity, respectively, at a given temperature. Oxygen transport numbers are very low in the temperature range studied, decreasing steadily from ~0.05 at 769 °C to only ~0.01 at 505 °C.

Conclusions

A highly promising high-temperature proton conductor, $SrCe_{0.95}Yb_{0.05}O_{3-\delta}$, has been studied using impedance spectroscopy under dry O_2, wet O_2 and wet H_2 atmospheres, over the range 850–300 °C. Above ~550 °C, the material shows higher conductivity in dry O_2 than in wet O_2 or wet H_2, while in wet atmospheres the values obtained for each temperature are similar; below that temperature the results obtained for the three atmospheres are almost the same. The activation energy in dry O_2 (0.77 eV) is higher than the activation energies in wet O_2 and wet H_2 (0.62 eV).

Moreover, oxygen tracer diffusion coefficients (D^*) and surface exchange coefficients (k) have been measured using $^{16}O/^{18}O$ IEDP/SIMS, in the temperature range 500–800 °C. The values of D^* and k increase steadily with temperature. Oxygen ion conductivities have been calculated using D^*, by means of the Nernst–Einstein equation. The values obtained are at least one order of magnitude lower than the conductivity data in dry O_2 obtained by impedance spectroscopy in that temperature range, with transport numbers for oxide ions almost negligible. This suggests that oxygen conduction is irrelevant for the temperatures studied, and that hole conduction dominates at high pO_2 in this temperature range.

Acknowledgements This project has been funded by the EU Research Training Network "HiT Proton" (HPRN-CT-2000-00042). M.S. is grateful to the Royal Academy of Engineering for the award of a research fellowship.

References

1. Iwahara H, Esaka T, Uchida H, Maeda N (1981) Solid State Ionics 3/4:359
2. Bonanos N, Ellis B, Mahmood MN (1988) Solid State Ionics 28–30:579
3. Kosacki I, Becht JGM, van Landschoot R, Schoonman (1993) Solid State Ionics 59:287
4. Krug F, Schober T, Springer T (1995) Solid State Ionics 81:111
5. Matsumoto H, Iida Y, Iwahara H (2000) Solid State Ionics 127:345
6. Hibino T, Hashimoto A, Mori K, Sano M (2001) Electrochem Solid State Lett 4(5):H9
7. van Rij LN, van Landschoot RC, Schoonman (2001) J Sens Actuators B 75:111

8. van Rij LN, Lee J, van Landschoot RC, Schoonman J (2001) J Mater Sci 36:1069
9. Oghi T, Namikawa T, Yamazaki Y (1993) In Poulsen FW, Bentzen JJ, Jacobsen T, Skou E, Østergård MJLQ (eds) Proceedings of the 14th Risø international symposium on materials science. Risø National Laboratory, Roskilde, Denmark, pp 357–362
10. De Souza RA, Kilner JA, Steele BCH (1995) Solid State Ionics 77:180
11. De Souza RA, Kilner JA (1997) Solid State Ionics 97:409
12. Knight K, Bonanos N (1995) Mater Res Bull 30:347
13. De Souza RA, Kilner JA (1998) Solid State Ionics 106:175
14. Chater RJ, Carter S, Kilner JA, Steele BCH (1992) Solid State Ionics 53/56:859
15. Kosacki I, Tuller HL (1995) Solid State Ionics 80:223
16. Iwahara H (1996) Solid State Ionics 86/88:9